Two-dimensional color correction: Recent advances

Vishal Monga and Raja Bala, Xerox Research Center Webster, NY, USA

Abstract

Color device calibration is the process of achieving and maintaining a desired color response. For printers, calibration is typically achieved via 1-D tone reproduction `curves (TRCs) applied to each of C, M, Y and K colorant channels. This however, can be severely restrictive in the amount of control. For example, 1-D TRCs can be designed for either gray-balance or smooth rendition of individual color ramps, but not both. To enable complete control, 3-D/4-D color transforms may be used but they are at odds with the goal of calibration being a lightweight transform with respect to measurement and computation. In 2004, Bala et al. proposed two-dimensional (2-D) calibration to facilitate a superior cost vs. control trade-off. In this paper, we view the design of cost-effective calibration transforms as a dimensionality reduction problem. We observe that the quality of the transform, i.e. its ability to match a true higher-dimensional (4-D) transform, depends on both the projection operator applied to high-dimensional device inputs, and the functional approximation built out of the reduced dimension variables. With that view, we develop techniques to significantly enhance the accuracy of previously proposed 2-D calibration transforms. In particular, we develop 2-D color transforms that allow complete control of cleverly selected 2-D planes in the 3-D CMY cube. We also develop a novel 2-D calibration LUT for the K channel which exploits the knowledge of printer GCR strategy to improve rendition of dark colors. Experimental results show vastly improved calibration ability particularly for the case of calibrating multiple devices to a common colorimetric aim.

Key words: color calibration, dimensionality reduction, color control.

1. Introduction

Color management for output devices is commonly partitioned [1] into a characterization and a calibration transform. As an example for a four color CMYK printer, the characterization transform is a multidimensional correction that maps device independent colors (e.g. CIELAB) to device dependent CMYK colors. The calibration transform is a mapping in device dependent space (e.g. from CMYK to C'M'Y'K') that maintains a desired printer response. This paper focuses on CMYK printer calibration. Since calibration is carried out frequently, it is desirable to make this process inexpensive and easy to execute. Additionally, the calibration transform is required to be computationally efficient with a reasonable memory requirement so that it can be incorporated in high-speed real-time printing paths.

Calibration architectures vary in the degree of control they provide and the underlying cost i.e. required measurements, storage and/or computation. Traditional one-dimensional (1-D) calibration implemented by using simple 1-D LUTs from CMYK to C'M'Y'K' is the most cost effective, but also significantly limits the control available over the device color gamut. A typical example of this limited control is that 1-D TRCs in a printer can be used to either ensure gray balance along the C = M = Y axis or to provide a linear response in delta-E units along each of the individual (C, M and Y) axis, but not both. On the other hand, 3-D or 4-D calibration transforms enable significantly more control but tend to require prohibitively large measurements, storage and/or real-time computation. As an intermediate alternative, multi-axis two-dimensional (2-D) calibration transforms [2] have been developed that allow control of multiple 1-D device axes, e.g. both neutral (C=M=Y) and individual colorants. 2-D calibration has been shown to offer an appealing trade-off between quality (i.e. control, accuracy) and cost (i.e. measurement, storage, computation).

This paper views 2-D calibration formally as a dimensionality reduction problem. First, we observe that although 4-D calibration is somewhat impractical, a true 4-D transform can be used as a conceptual benchmark for all lower-dimensional calibration transforms. Then, it follows naturally that the quality of a lower-dimensional, e.g. 2-D calibration transform would depend on both the projection operator applied to the 4-D CMYK vector, and the functional approximation built out of the reduced dimension variables. With this insight, we develop 2-D color calibration transforms that allow superior control over the device color space, while incurring modest overhead in measurement and computational cost. In particular, we develop 2-D color transforms that allow complete control of selected 2-D planes in the 3-D CMY cube. This is superior to previous calibration methods that enable control over multiple 1-D loci rather than entire 2-D planar regions. We also develop a novel 2-D calibration LUT for the K channel which exploits the knowledge of printer GCR strategy to improve rendition of dark colors.

2. Review of Printer Calibration Transforms

1-D Calibration: Traditionally, calibration takes the form of one-dimensional tone reproduction curves (TRCs) applied to the individual C, M, Y, K channels, i.e. C' = f_1(C), M' = f_2(M), Y' = f_3(Y), K' = f_4(K).

Cost vs. control: Small number of measurements is required

by sampling colors along the 1-D locus of interest. Memory requirements are also minor: for 8-bit processing, each 1-D LUT 256 bytes of memory for each separation. The control is severely restricted though; common example is the grey-balance vs. channel-wise linearization trade-off.

3-D or 4-D lookup table based calibration[1]: This means constructing calibration transforms of the type:

C' = f₁(C, M, Y), M' = f₂(C, M, Y), Y' = f₃(C, M, Y) or C' = f₁(C, M, Y, K), M' = f₂(C, M, Y, K), Y' = f₃(C, M, Y, K), K' = f₄(C, M, Y, K).

Cost vs. control: Cost for 3-D/4-D calibration becomes similar to characterization, typically involving a large number of measurements, large LUTs and multi-dimensional interpolation (more computation). Clearly, complete control of the 3-D/4-D device space is possible.

Multi-axis 2-D calibration: This is implemented by first constructing two-dimensional intermediate variables from 3-D/4-D device values. An example is shown in Fig. 1. (In this instantiation, K is processed separately through the conventional 1-D calibration transform.)

Cost vs. control: This approach provides the opportunity for a better cost-control trade-off. Clearly, 2-D LUTs in Fig. 1 are larger than 1-D LUTs - 128 Kb vs. 256 bytes, but still much smaller than 3-D/4-D LUTs, which are of size 16 MB and 4.2 GB respectively. In [2], Bala et al. demonstrated better control than 1-D calibration by calibrating multiple 1-D loci in the 2-D tables in Fig. 1. A key example is simultaneous control along the primary colorant channels as well as the device neutral axis (the diagonal line through each of the C, M and Y tables).

3. Dimensionality reduction for calibration – A framework

In Ref [2] Bala et al. demonstrated how using an intermediate dimensionality, i.e. 2-D, could enable a much better cost quality trade-off over conventional calibration transforms. We now formulate the problem for deriving an optimal lower-dimensional calibration transform. Let X represent the "higher-dimensional" space of device colorant variables, e.g. for CMYK printers, a particular **x** in X is a 4-D vector comprising of C, M, Y and K values. And let the true higher-dimensional calibration transform be given by f such that

$$f : X \rightarrow Y \qquad (1)$$

---

[1] Such calibration transforms are not commonly used but are included here for completeness and for conceptual importance to the proposed work.

where **y** in Y represents the output of the calibration transform, e.g. **y** = [C' M' Y' K'].
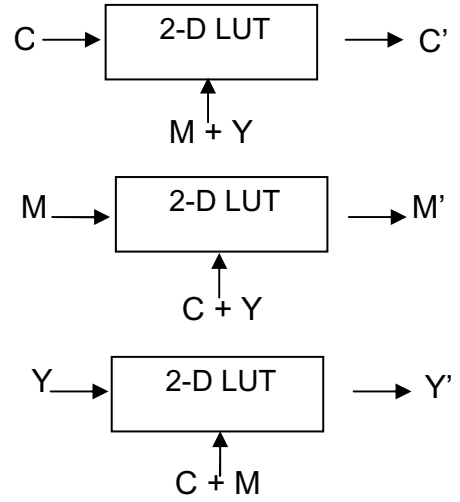
Figure 1: Example of 2-D calibration as proposed by Bala et al. [2]

Then the lower-dimensional calibration problem can be formulated as the design of a projection operator *P* and a function g( ) such that

$$(P^*, g^*) = \arg\min_{(P,g)} \oint_X \|f(\mathbf{x}) - g(\mathbf{\theta})\|^2 d\mathbf{x} \quad,$$

$$\text{where } \mathbf{\theta} = P(\mathbf{x}) \qquad (2)$$

That is, **θ** is the projection of **x** on to a lower-dimensional space Θ.

The 2-D calibration LUTs presented in the previous subsection may now be understood as the instantiation of the general framework in Eqn (2) for the case when separate projection operators were designed for the C, M and Y channels. In particular, **θ** is a set of 3 projection operators, [**θ**ₓ, **θ**ₘ, **θ**ᵧ] where **θ**ₓ = [C, M + Y], and analogous expressions hold for **θ**ₘ and **θ**ᵧ .

The formulation of Eqn. (2) reveals that there are two factors that determine the quality of the low-dimensional calibration: 1.) the projection operator *P,* and 2.) the actual calibration function g(.) defined on variables in the lower dimensional space. To fix ideas for 2-D calibration look up tables, g() = [gₓ gₘ gᵧ] represent the values that are filled in the C, M and Y 2-D look up tables respectively.

Eqn (2) suggests that with a reasonable quantitative description of the 4-D transform being available; we can use search based methods [3] to solve for the "optimal" projection operator. In practice however, the design of the projection operator is limited by the physical nature of the input variables as well as real-time constraints on processing. For example, note that the intermediate variables that are inputs to the 2-D look up tables in Fig. 1 cannot be

made arbitrarily complex because they would have to be computed in real time for every input CMY(K) color to be mapped through the calibration transform.

With the dimensionality reduction framework of Eqn (2) in view, this paper presents novel 2-D calibration transforms. In the first advancement presented in Section 4, novel approximation functions [g_c g_m g_y] are derived. Section 5 then presents a new projection operator **P** applied to the CMYK device vector to create intermediate 2-D variables that index a 2-D LUT for K.

4. Device Calibration with Planar Control

We retain the same projection operator for the CMY 2-D tables, i.e. intermediate 2-D variables as in Fig. 1. Our work then focuses on constructing g()'s based on controlling 2-D planes in the 3-D CMY cube.

(a)

(b)
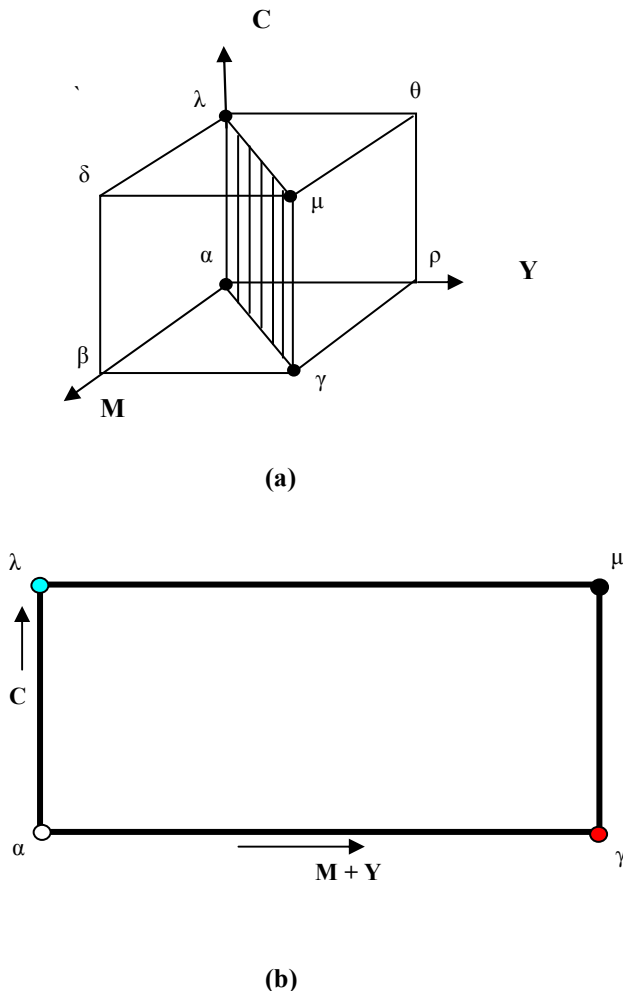
Figure 2: (a) The primary 2-D plane used for the cyan LUT, (b) Projection onto cyan 2-D LUT.

First we select a primary plane for accurate control. Fig. 2 (a) shows one example of such a plane that intersects

with white, cyan, black, and red vertices in the CMY cube. Fig. 2 (b) shows the projection of this plane onto the cyan 2-D LUT. Note that the chosen primary plane projects onto the entire domain of the cyan 2-D LUT. The same primary plane must then be projected onto the 2-D LUTs for magenta and yellow. These are shown in Figs. 3-4. Note that the chosen primary plane only projects onto a fraction of the domain for the magenta and yellow 2-D LUTs. The remaining portions of these 2-D LUTs can be used for controlling additional secondary planes, as shown in Figs. 4 (a) and (b).

Populating the Calibration Tables

The 2-D LUTs are derived with the purpose of maintaining a fixed defined CIELAB aim within the primary and secondary planes described above. This aim could be the printer's response at some reference state, the aggregate response of a fleet of similar devices, or the response of a standard device (e.g. SWOP press). We populate each of the tables by solving a printer-model inversion problem, which obtains C, M, Y, K amounts required to produce a certain CIELAB color.

(a)

(b)
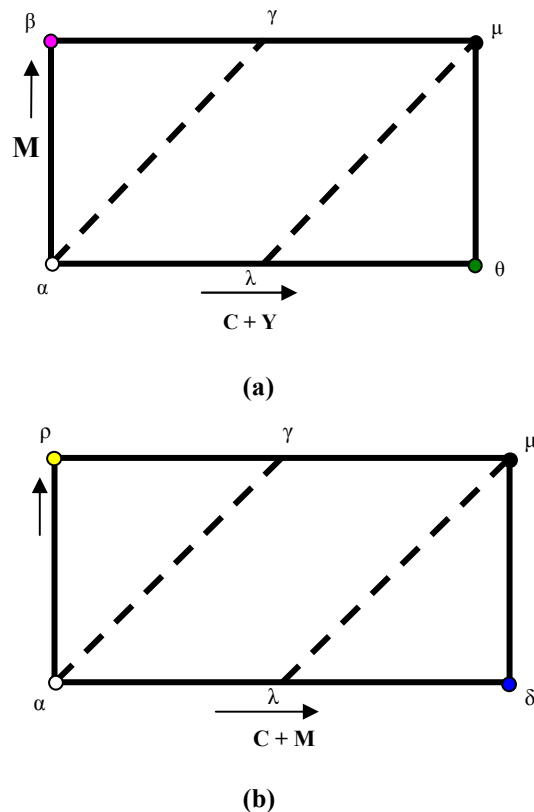
Figure 3: (a) The Magenta 2-D LUT. Note the vertices define the planar regions in the CMY cube in Fig. 4 (a), and (b) Yellow 2-D LUT; vertices define the planar regions in the CMY cube in Fig. 4 (b).
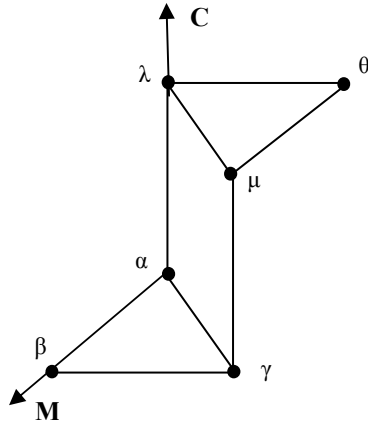
(a)
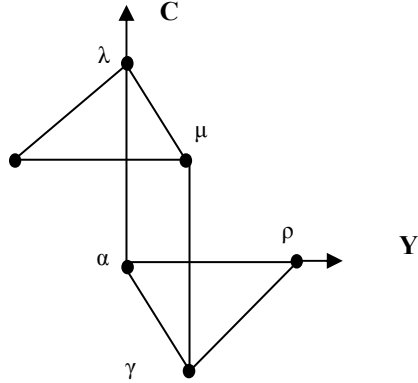
(b)

Figure 4: (a) Primary and secondary 2-D planes that manifest in the Magenta 2-D LUT, (b) Primary and secondary 2-D planes in the Yellow 2-D LUT.

This inversion can be stated as follows:

$$(C', M', Y') = \underset{C,M,Y \in [0,255]}{\arg\min} \left\| \mathbf{c}_0 - \mathbf{c} \right\|_2$$

$$where \ \mathbf{c}_0 = (L_0, a_0, b_0)^T$$

$$and \quad \mathbf{c} = (L, a, b)^T = pm(C, M, Y) \quad (3)$$

$\mathbf{c_0}$ represents the vector of aim CIELAB values for the CMY being calibrated and $\mathbf{c}$ represents the output CIELAB vector from a printer-model describing the printer to be calibrated.

In practice, such a printer- model can be made by using measurements from the calibration targets. Preferably, the

targets should contain CMYK patches chosen in the vicinity of the planes being calibrated. For more details, we refer the reader to [2]. Note here that the (C, M, Y) that lie on the primary diagonal plane in Fig. 2 manifest in each of the C, M and Y calibration LUTs allowing for a joint population of these LUTs. This ensures that the desired CIELAB color for all CMY on this plane is achieved. This is in contrast to previous multi-axis 2-D calibration schemes where most of these colors would be determined by an interpolation between a few selected 1-D axis that lie on this plane. In the context of the framework of Section 3, this means that the g() defined over these planar regions in 2-D table is in exact agreement with the 4-D calibration transform f, whereas in the multi-axis 2-D approach [1] this exact agreement is over a much smaller set of colors, viz. certain 1-D loci that lie on this plane.

5. 2-D calibration LUT for K

Thus far the K channel is still handled by a 1-D transform. The interaction of K with CMY can however be crucial, e.g. for accurate rendition of dark colors. We propose the use of a 2-D look up table for calibrating the K channel. The reduced dimension 2-D vector (after projecting from CMYK) is defined as $\theta = [\theta_1 \ \theta_2] = [K, \min (C,M,Y)]$. We choose K as one of the axes to enable control along the pure K channel. The choice of min(C, M, Y) for the other intermediate variable was motivated by two primary reasons: 1.) min(C, M, Y) is an intuitive estimate of the "gray component" in the CMY mixture and 2.) printer grey-component replacement (GCR) [1] strategies that are crucial to the interaction of CMY and K typically use min(C,M,Y) to determine the amount of K substitution as well as the subtraction of C, M, and Y.
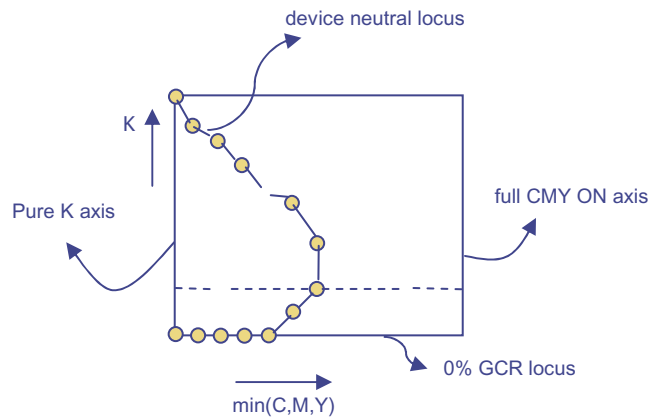
Fig. 5 Critical loci of interest in the 2-D calibration table for K

Populating the 2-D LUT for K (determining g())

Our basic strategy is to identify certain principal loci of interest in the 2-D table, derive corrections (i.e. K') for those loci and then use simple linear interpolation to fill in

the rest of the table. The principal loci are shown in Fig. 5 and defined as:

1. "Pure K axis": K increasing from 0-255 (in steps of 1 for 8-bit digital processing) and C = M = Y = 0; conceptually this may also be understood as the 100% GCR axis because no CMY is present.
2. "True device neutral locus": This locus is obtained as follows: process d = C=M=Y, (d in [0,255]) sweep through a GCR function suitable for a given device to produce $(\overline{C}, \overline{M}, \overline{Y}, K)$. Then K vs. $\min(\overline{C}, \overline{M}, \overline{Y})$ spans a 2D locus representing the true device neutral. Conceptually, we refer to it as a locus of intermediate GCR.
3. "0% GCR locus": This locus is described simply by C=M=Y=d, (d in [0,255]) sweep with K = 0.
4. "Full CMY ON axis" : this is the 1-D axis given by C=M=Y=255, K increasing from 0-255

The goal is to derive corrections to achieve a desired device-independent response (in CELAB coordinates) along each of these loci.

- The pure K axis may be populated simply by linearizing to a metric like deltaE from paper as in traditional 1-D calibration.
- Full CMY ON axis: Note that the upper right hand corner of the 2-D table for K in Fig. 5. is trivially set to the max possible K (255 for 8 bit processing). We assume for the moment that the calibrated K value at C=M=Y=255 and K=0 is also available (this value comes from populating the "0% GCR" locus which will be explained shortly). The full CMY ON axis may then be populated by a simple interpolation technique between these corner points.
- "True device neutral locus": This locus is made up of K vs. $\min(\overline{C}, \overline{M}, \overline{Y})$ pairs that result from running an equal CMY sweep through the GCR. Two crucial observations need to be made here: 1.) GCR strategies along the neutral axis preserve the neutrality of the C, M, Y samples, i.e. the resulting CMYK also has $\overline{C} = \overline{M} = \overline{Y}$, and 2.) deciding what K to fill in must factor in that these $(\overline{C}, \overline{M}, \overline{Y})$ values get processed through their respective C, M and Y calibration transforms. As illustrated in Fig. 6, calibrating this locus amounts to finding the K' values that will satisfy a desired CIELAB response when combined with the C', M' and Y' (calibrated C, M, Y) values. Further, because this is the neutral axis the aim is defined completely by a one dimensional locus of L* values.
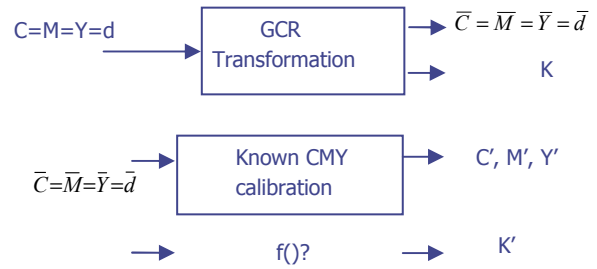
Fig. 6: Calibrating the true device neutral locus in the 2D table for K

Let g(.) represent our desired L* locus as a function of the digital level d in [0, 255]. Then the calibrated K' along this locus is determined as

$$K'(d) = \underset{K \in [0,255]}{\arg\min} \left\| pm_{L*}(C', M', Y', K) - g(d) \right\|_2$$

$$\text{for each } d \in [0,255] \qquad (4)$$

where pm(C,M,Y,K) represents a Negueabuer printer model that provides a mapping from printer CMYK to CIELAB values. Further, $pm_{L*}(\ )$ signifies that the L* value is used.

- The "0% GCR locus" may then be populated in a manner similar to the "true device neutral locus" by searching for K' values to match another 1-D locus in L*.

Once these loci are populated, the rest of the table may be filled in using 1-D interpolation in the horizontal (i.e. min (C,M, Y)) direction as shown in Fig. 5.

6. Preliminary Results

6.1 Planar Control:

We compare 3 different calibration methods:

1. *Traditional 1-D calibration:* 1-D gray-balance calibration for C, M and Y and a 1-D deltaE from paper linearization calibration for K.
2. *Multi-axis 2-D calibration* [2] based on interpolating between several 1-D axes.
3. *2-D planar calibration* as detailed in Section 4.

We evaluate various calibrations for their ability to match the color response of a fleet of color devices. The devices in this experiment were three Xerox color laser printers which we will refer to as A, B and C. For each of the calibration methods, any device (A, B or C) was calibrated to match a common CIELAB aim. For 1-D calibration, this aim was defined for the neutral axis, for multi-axis 2-D calibration this aim was defined for each of the 1-D axes in the 2-D

LUTs, and for the proposed method in this invention the aim was defined for the CMY values corresponding to the selected planar regions. Table 1 shows the pair-wise deltaE errors between printers A and C when they were calibrated using different calibration methods.

Calibration Method	Average ΔE	95th percentile ΔE	Maximum ΔE
1-D gray-balance calibration	1.65	4.66	6.07
Multi-axis 2-D calibration	1.31	2.08	4.47
2-D planar calibration	0.94	1.89	3.02

Table 1. Pairwise ΔE errors for fleet calibration: A vs. C

6.2   2D LUT for K: Improved accuracy in rendering dark colors

To evaluate the ability to render dark colors we start with a CIELAB target of in-gamut colors corresponding to low luminance values (and hence substantial input K) and use the (inverse) characterization to obtain the CMYK which are subsequently processed through each of the respective calibrations and then printed and measured. The deltaE difference of measured vs. the original Lab values gives an evaluation measure for the calibration. We used 216 randomly generated Lab values (corresponding to dark colors) for this test. Table 2 shows how each calibration fares in terms of matching the original desired Lab.

7.   Conclusion

This paper presents recent advances in two-dimensional printer calibration. We formulate calibration as a dimensionality reduction problem. In this framework, the design of calibration transforms is a two-step process: 1) determine a projection operator applied to the 4-D CMYK space to yield lower-dimensional variables, and 2) design a functional approximation to the true 4-D calibration transform, where the function is evaluated on the lower-dimensional variables. Previously known 1-D and 2-D calibration transforms are therefore interpreted as specific instantiations of our general framework. We then employ this novel perspective to formulate the design of 2-D calibration transforms as a constrained optimization problem. Geometrically, our newly developed transforms are superior in the sense that they enable control of 2-D planar regions, whereas existing methods only allow control

Calibration Method	Average ΔE	95th percentile	Maximum ΔE
1-D gray-balance	3.21	6.11	8.02
1-D gray-balance for CMY, 2-D for K	2.21	4.98	6.55
Multi-axis 2-D CMY w 1-D for K	2.83	4.72	6.80
2D CMY w 2D for K	2.01	4.55	5.69

Table 2. Evaluating different calibrations for rendition of dark colors

of multiple 1-D loci. In addition to greater accuracy, the methodology proposed in this paper also allows greater flexibility in the design of calibration transforms viz. by picking different primary and secondary planes. The 2-D calibration for K demonstrates superior control in neutral regions. While we apply these techniques to printing devices, we believe they will be quite useful for additive RGB displays as well.

8.   References

1. R. Bala, "Device characterization", Chapter 5 of *Digital Color Imaging Handbook*, Gaurav Sharma Ed., CRC Press, 2003.
2. R. Bala, V. Monga, G. Sharma and J. P. V. Capelle, "Two-dimensional Transforms for Device Color Calibration", *Proc. SPIE: Color Imaging IX: Processing Hardcopy, and Applications,, vol. 5293*, pp. 250-261, San Jose, 2004.
3. Dimitri P. Bertsekas, *Nonlinear Programming,* Athena Scientific, 2002.

Author Biography

Vishal Monga is a Member of Research Staff at the Xerox Research Center Webster in Webster, NY. He received his B. Tech degree from Indian Institute of Technology in May 2001 and his M.S. and PhD degree in Electrical Engineering from The University of Texas at Austin in May 2003 and Aug 2005 respectively. His research interests lie broadly in statistical signal and image processing. He has researched problems in color imaging, multimedia security and mining. In color imaging, his interests span a variety of processing blocks in the printer and digital camera pipeline with the common underlying theme being opportunities for non-separable processing of color planes.